doi:10.1007/s11589-012-0828-4

Shear-wave splitting beneath Yunnan area of Southwest China*

Yutao Shi[1,2,♦] Yuan Gao[1,2] Youjin Su[3] and Qiong Wang[2]

[1] *Institute of Geophysics, China Earthquake Administration, Beijing* 100081, *China*
[2] *Institute of Earthquake Science, China Earthquake Administration, Beijing* 100036, *China*
[3] *Earthquake Administration of Yunnan Province, Kunming* 650041, *China*

Abstract Systematic analyses of seismic data recorded by the Yunnan regional seismograph network reveal significant crustal and upper mantle anisotropy. Splitting of the S phase of local earthquakes and teleseismic SKS, PKS, and SKKS phases indicates time-delays from 1.60 ms/km to 2.30 ms/km in the crust, and from 0.55 s to 1.65 s in the upper mantle which corresponds to an anisotropic layer with a thickness about between 55–165 km. The polarization orientations of fast shear waves in the crust are complicated with a predominantly north-south direction, and the mantle anisotropy has a nearly west-east direction. Our results show different deformation styles and mechanisms exist between the crust and upper mantle.

Key words: **seismic anisotropy; polarization orientation; principal compressive stress; shear wave; SKS, PKS and SKKS**

CLC number: P315.3, P315.63 **Document code**: A

1 Introduction

Seismic anisotropy is a universal phenomenon in the crust and upper mantle. It is becoming increasingly important in our understanding of the structure, deformation, and dynamics of the Earth's crust and mantle. Shear-wave splitting can be used to study seismic anisotropy in the crust formed by vertically parallel arrangement cracks (Crampin, 1984; Crampin and Atkinson, 1985) and other structures, to analyze crust stress condition, and to describe the static and dynamic states of the related anisotropy parameters (Gao et al., 1999; Zheng et al., 2008). In the upper mantle, lattice-preferred orientation of crystallographic axes of elastically minerals, such as abundant olivine, dominates the anisotropic structure (Silver and Chan, 1991; Savage, 1999). Numerous studies indicated that seismic anisotropy is related to lithospheric fabrics and mantle flow, as demonstrated in the vicinity of mid-ocean ridges (Hess, 1964). The splitting of P-to-S converted phases at the core-mantle-boundary, especially the SKS phase, is most effective for characterizing upper mantle anisotropy beneath the seismic stations (Kind et al., 1985; Silver and Chan, 1991).

It is generally accepted that the polarization direction of the fast shear-wave indicates the direction of the principal compressive stress of the crust beneath the seismic station, and the time-delays of shear-wave splitting bring with information of stress accumulation and temporal variation in the crust. Consequently, it is possible to use shear-wave splitting to monitor the characteristics of crustal stress field and to forecast the occurrence of earthquakes (Crampin, 1978; Gao and Crampin, 2004). Complex geologic structure can result in azimuthal and spatial variations of splitting parameters (Gao et al., 1995, 1999; Lei et al., 1997; Zhang et al., 2009). Shear-wave splitting is a significant manifestation of seismic anisotropy in the mantle and thus can provide an important insight into the structure and deformation of the crust and upper mantle. Both lithospheric deformation (Silver, 1996; Gao and Liu, 2009) and asthenospheric flow (Vinnik et al., 1995; Gao et al., 1994) can lead to observed mantle anisotropy. It is possible that different regions are dominated by different mantle deformation. An excellent example of litho-

* **Received** 30 September 2011; **accepted in revised form** 16 December 2011; **published** 10 February 2012.
♦ **Corresponding author. e-mail**: shiyt@seis.ac.cn

spheric deformation is the Tibetan plateau, while western North America is dominated by asthenospheric flow (Silver, 1996; Gao and Liu, 2009).

This study aims at measuring crustal and mantle anisotropy beneath the Yunnan area in southwestern China. The study area is located in the southeast region of the Tibetan plateau and is part of North-South Seismic Zone (Figure 1). Seismically, the area is one of the most active intra-continental areas on Earth, as evidenced by the numerous magnitude 5 or greater earthquakes (Figure 1). This study uses local and teleseismic data from the Yunnan regional seismograph network to characterize crustal and mantle anisotropy by shear-wave splitting so as to explore the mechanisms responsible for the observed anisotropy, and to investigate the relationship between crustal and mantle anisotropy.

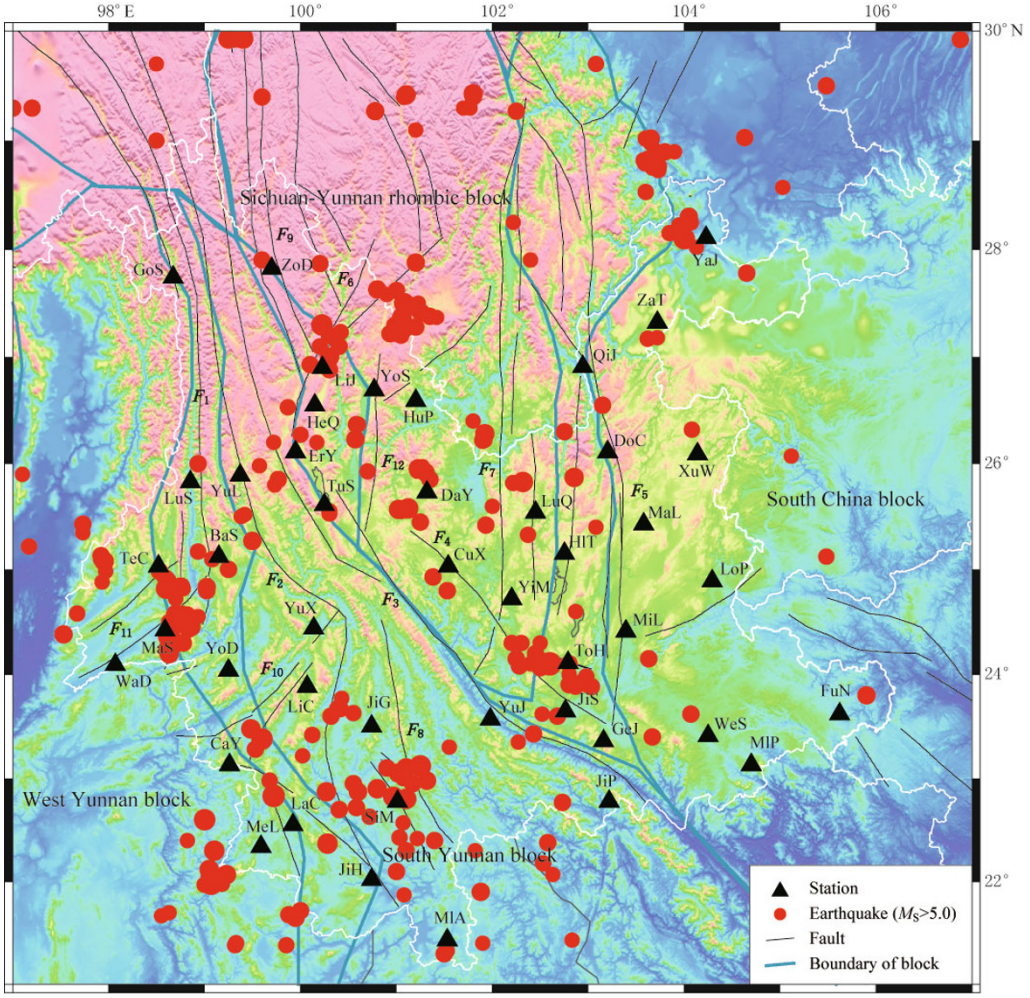

Figure 1 Topographic map of the study area showing spatial distribution of seismic stations, earthquakes, major faults and tectonic blocks. F_1. Nujiang fault; F_2. Lancangjiang fault; F_3. Honghe fault; F_4. Chuxiong-Tonghai fault; F_5. Xiaojiang fault; F_6. Lijiang-Jianchuan fault; F_7. Yimen fault; F_8. Wuliangshan fault; F_9. Zhongdian fault; F_{10}. Nandinghe fault; F_{11}. Longling fault; F_{12}. Chenghai fault.

2 Regional geological setting

Major tectonic features of the study area are dominated by the collision between the Indian and Eurasian plates. Major faults in the study area are of right-lateral strike-slip faults such as the Honghe, Nujiang and Xiaojiang faults (Deng et al., 2002). Most of the faults to the east of the Honghe fault are mainly N-S or NE oriented, while in the western region they are mostly NW oriented. GPS studies revealed present-day intensive crustal deformation in the study area. Crustal strain measurements and focal mechanism solutions indicated that the principal compressive stress axis of the Yunnan area is nearly N-S (Han et al., 1977, 1983; Wu et al., 2004).

Based on GPS and other observations, the study area is divided into Sichuan-Yunnan rhombic block, west Yunnan block, south Yunnan block and part of South China block (Figure 1). The thickness of the crust beneath the northwest part of the study area is approximate 62 km and reduces to about 32 km in southeast area. Heterogeneities in crustal thickness and shear-wave velocity (Wu et al., 2001) result in complicated crustal deformation patterns (Figure 1).

3 Methods

Splitting of shear-waves originated from local earthquakes is quite sensitive to crustal anisotropy. The propagating shear-wave traveling through an anisotropic medium is split into two quasi shear-waves with orthogonal polarizations and different velocities. The polarization of the fast shear-wave is parallel to the vertically aligned micro-cracks, while the polarization of slow shear-wave is nearly perpendicular to the aligned micro-cracks. Theoretically, due to originating from the same source, the waveforms of the fast and slow shear-waves are similar. Therefore, the method of correlation analysis is used in order to estimate the splitting parameters (Gao et al., 1995). The shear-wave splitting system analysis method, SAM method (Gao et al., 2004), is used in this study. The technique includes computation of the three components, cross-correlation function calculation, elimination of the effect of time-delay and analysis of polarization. This method has the function of self examination (Gao et al., 1994; Gao et al., 2004).

By eliminating the effect of the time delay and rotating the orientation polarization, we find a nearly linear feature in the polarization (Figure 2).

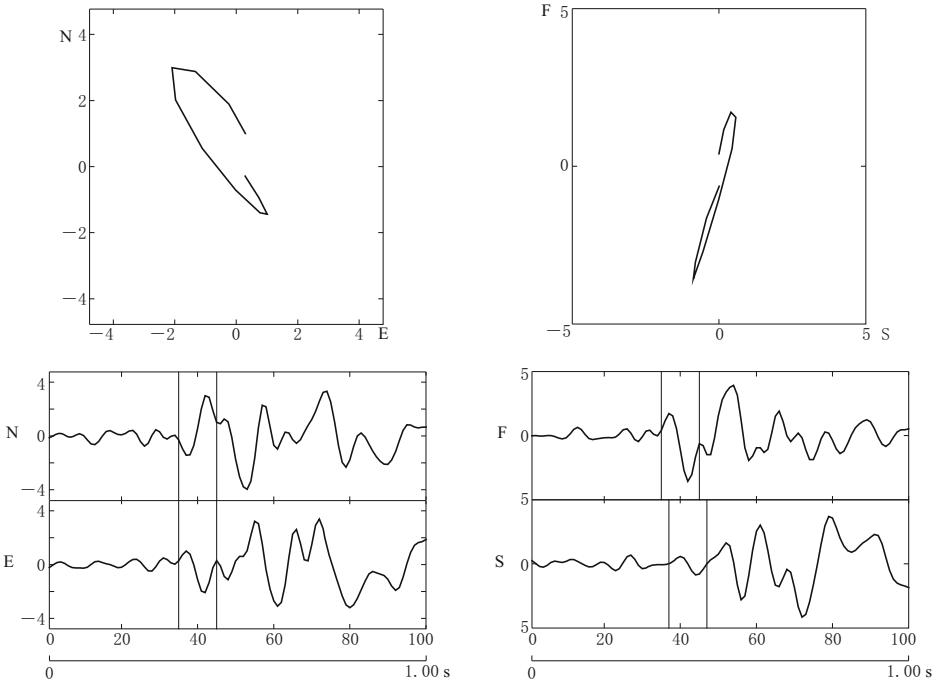

Figure 2 Analysis of system analysis method (SAM). The data was recorded on December 17, 2009 by TuS station, the focal depth is 7.0 km, and the magnitude is M_L1.1. The sampling rate of data is 100. The left shows the horizontal shear-waves with north (N) and east (E) components (bottom), and the polarization of two horizontal shear-waves (top). The right shows the fast (F) and slow (S) shear-wave waveform (bottom), and the polarization of fast and slow shear-waves without the effect of time-delay. The erected lines indicate the arrival of shear-wave (left panel), and the arrivals of fast shear-wave and slow shear-wave (right panel). The ordinate is the count value of amplitude, and the abscissa is the number of sampling points in the bottom waveform picture.

Mantle anisotropy is mostly caused by lattice preferred orientation of crystallographic axes of olivine, which composes about 60% of the Earth's upper mantle. Polarization of the fast shear-wave is parallel to the olivine a-axis direction which is aligned parallel to the direction of asthenospheric flow or orthogonal to the direction of lithospheric shortening. The time delay between the fast and slow waves is proportional to the

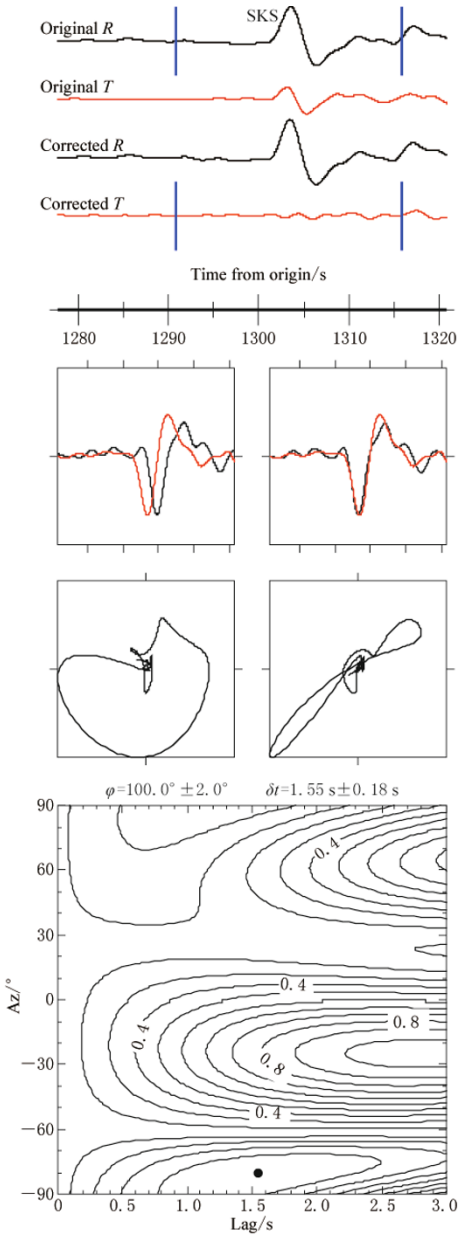

Figure 3 Shear-wave splitting analysis using an SKS phase for the station JiP. For the station JiP (22.8°N, 103.2°E), backazimuth is 118.781°, epicentral distance is 88.252 km. The event occurred at 21:05 on 2007-289 with its epicenter (25.77°S, 179.53°E) with focal depth 509.0 km. The top panel shows the original and corrected radial and transverse components, the middle panel shows the resulting fast and slow components and the corresponding particle motion patterns, and the bottom shows the contour diagram of the energy on the corrected transverse component.

product of the magnitude and thickness of the anisotropic layer. This study uses high-quality XKS (including PKS, SKKS, and SKS) data from teleseismic events with M_S>6.0 to measure the anisotropic parameter of the upper mantle of Yunnan area. The seismic data were band-pass filtered in the frequency range of 0.04 Hz to 0.5 Hz to improve the signal quality. The optimal pair of XKS splitting parameters is measured by the grid searching method of the minimum tangent energy (Silver and Chan, 1991; Gao et al., 1994; Liu et al., 2008; Liu, 2009). The use of multi-event stacking procedure confirms the optimum values of splitting parameters (Wolfe and Silver, 1998) (Figure 3).

4 Results of shear-wave splitting analyses

Data from 46 digital seismic stations in the Yunnan regional seismograph network (Zheng et al., 2010) are used in the study. When the shear-wave encounters the free face, there will be total reflection if the incidence angle is larger than the critical angle, which is about 35° for the Poisson medium and is also the limited range of the shear-wave window. According to the velocity structure of the shear-wave of Yunnan area (Wu et al., 2001), the data with 37° shear-wave window was adopted for crustal anisotropy from January 2000 to October 2010. The anisotropic parameters were obtained using 709 local earthquakes, recorded at 32 stations with more than three effective records in the shear-wave window. The broadband seismic data used for the measurement of mantle anisotropy were recorded from August 2007 to October 2010. The 284 shear-wave splitting results consist of 183 SKS phases, 71 PKS phases and 30 SKKS phases recorded by 37 broadband stations. Stations with three or more reliable measurements were used for anisotropic analysis. The shear-wave splitting results of all stations are listed in Table 1.

According to the statistics, the average polarization directions in the crust are northwest direction beneath twelve stations (BaS, CuX, DaY, ErY, LaC, LuS, ToH, TuS, WeS, YoD, YuX, ZaT), nearly northeast direction beneath eight stations (GeJ, HlT, HeQ, JiS, LiJ, MaS, WaD, XuW), nearly north-south direction beneath nine stations (CaY, MaL, MlA, MiL, QiJ, TeC, YoS, YuJ, ZoD), and nearly east-west direction beneath three stations (DoC, LuQ, YiM). The time-delays of all stations fall into the range of 1.60–2.30 ms/km, and the deviations are 0.35 to 1.93 ms/km. The maximum and minimum values are 1.60 ms/km at YoD and 2.30 ms/km

Table 1 Splitting parameters for XKS phase and S phase

Station	Long./°E	Lat./°N	SKS, PKS and SKKS phase			Local S phase		
			Num	Polarization± error/°	Time-delay± error/°	Num	Polarization± error/°	Time-delay± error /(ms·km^{-1})
BaS	99.2	25.1	–	–	–	70	147.3±33.4	2.30±1.90
CaY	99.3	23.1	6	109.0±8.9	1.06±0.22	41	5.2±26.1	1.80±1.30
CuX	101.5	25.0	5	112.6±6.3	1.28±0.23	55	144.9±40.5	1.90±0.90
DaY	101.3	25.7	5	102.4±14.3	0.92±0.68	3	160.0±10.0	1.80±0.90
DoC	103.2	26.1	3	103.0±16.5	0.55±0.19	6	82.5±24.9	1.80±1.00
ErY	100.0	26.1	7	69.3±14.0	1.14±0.38	26	150.6±28.3	2.20±1.60
FuN	105.6	23.6	5	87.8±7.6	1.13±0.18	–	–	–
GeJ	103.2	23.4	8	85.4±8.8	1.13±0.30	20	28.6±39.6	2.00±1.34
HlT	102.8	25.2	–	–	–	23	35.7±30.2	1.83±1.09
HeQ	100.2	26.6	–	–	–	131	23.9±30.2	2.13±0.93
GoS	98.6	27.7	6	119.8±9.3	1.08±0.38	–	–	–
JiG	100.7	23.5	11	102.5±6.9	1.32±0.42	–	–	–
JiH	100.7	22.0	6	110.3±8.2	1.22±0.32	–	–	–
JiP	103.2	22.8	14	94.0±8.29	1.39±0.33	–	–	–
JiS	102.8	23.7	6	90.0±7.92	1.23±0.25	3	20.0±10.0	2.09±1.80
LaC	99.9	22.6	3	134.3±8.8	1.05±0.29	5	124.0±23.0	1.81±1.32
LiC	100.1	23.9	10	110.6±5.2	1.54±0.29	–	–	–
LiJ	100.2	26.9	11	38.0±6.5	1.50±0.44	48	17.6±21.1	1.82±1.26
LoP	104.3	24.9	6	123.8±10.3	1.04±0.32	–	–	–
LuQ	102.5	25.5	5	30.2±4.6	1.35±0.41	8	97.5±29.6	1.94±1.43
LuS	98.9	25.8	6	99.2±7.1	1.44±0.33	29	159.1±34.9	1.77±1.07
MeL	99.6	22.3	3	101.0±9.8	1.08±0.42	–	–	–
MlA	101.5	21.4	16	93.50±7.8	1.00±0.24	3	170.0±20.0	1.71±0.95
MaL	103.6	25.4	–	–	–	3	6.7±15.2	1.78±1.09
MaS	98.6	24.4	–	–	–	4	26.3±18.8	1.79±1.08
MlP	104.7	23.1	3	74.7±9.2	1.12±0.32	–	–	–
MiL	103.4	24.4	4	46.5±6.0	1.33±0.36	17	8.2±17.4	1.67±0.95
QiJ	102.9	26.9				12	11.6±33.4	1.65±1.01
SiM	101.0	22.8	6	101.3±8.8	1.19±0.31	–	–	–
TeC	98.6	24.9	3	124.3±9.8	0.95±0.25	5	13.0±12.1	1.67±1.00
ToH	102.8	24.1	18	94.3±7.6	1.20±0.35	9	164.4±19.4	1.62±0.94
TuS	100.2	25.6	–	–	–	81	141.9±28.4	1.91±1.55
WaD	98.1	24.1	7	131.7±11.7	0.95±0.29	7	16.4±9.0	1.83±1.48
WeS	104.3	23.4	4	96.5±4.9	1.65±0.24	19	163.1±26.6	1.85±1.59
XuW	104.1	26.1	–	–	–	12	31.0±28.3	1.85±1.51
YaJ	104.2	28.1	6	140.8±7.3	1.27±0.26	–	–	–
YiM	102.2	24.7	17	91.2±8.8	0.97±0.24	28	72.6±37.9	1.54±1.04
YoD	99.3	24.0	5	117.2±8.8	1.34±0.33	11	142.7±19.4	1.60±1.05
YoS	100.8	26.7	19	73.0±8.0	1.10±0.28	15	12.3±15.9	1.61±1.06
YuM	101.9	25.7	4	80.0±7.8	1.11±0.26	–	–	–
YuJ	102.0	23.6	8	98.5±10.4	1.45±0.46	3	10.00±43.5	1.67±1.16
YaJ	99.4	25.9	14	66.9±11.1	1.12±0.33	–	–	–
YuX	100.2	24.4	5	114.8±13.7	0.88±0.33	14	135.00±45.40	1.63±1.14
ZaT	103.7	27.3	8	143.6±9.1	1.03±0.34	12	142.92±20.4	1.70±1.10
ZoD	99.7	27.8	11	109.8±5.9	1.30±0.26	4	171.25±6.29	1.72±1.12

at BaS, respectively.

Most stations show a dominant fast direction, as demonstrated by the rose diagrams (Figures 4 and 5). The average polarization orientations of fast shear-wave splitting obtained beneath most stations are nearly north-south, which are consistent with the principal compressive stress axis of Yunnan area. The average normalized time delay is 1.8±1.2 ms/km.

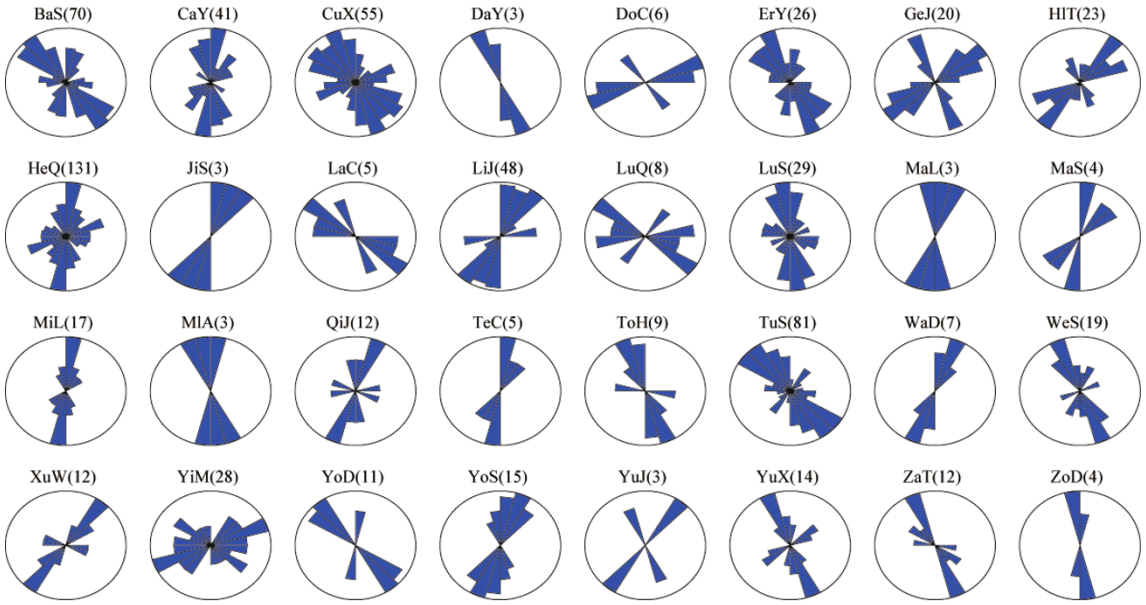

Figure 4 Rose diagrams showing resulting polarization directions of the fast shear-waves from local earthquakes. The circle represents the shear-wave window.

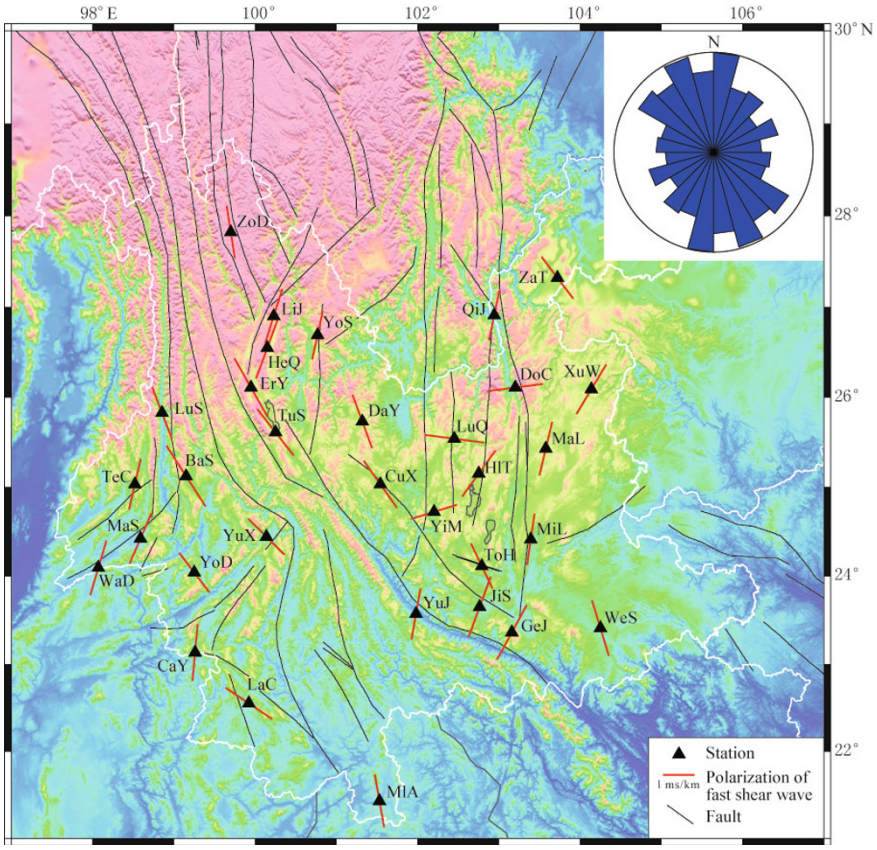

Figure 5 Resulting polarization directions of fast shear-waves from local earthquakes.

The resulting fast polarization directions from teleseismic XKS phases (Figure 6) show systematic spatial variations. Stations to the south of latitude approximately 25°N demonstrate nearly E-W fast directions which are at a high angle to the strike of most faults in the area. In contrast, those in the northern part of the

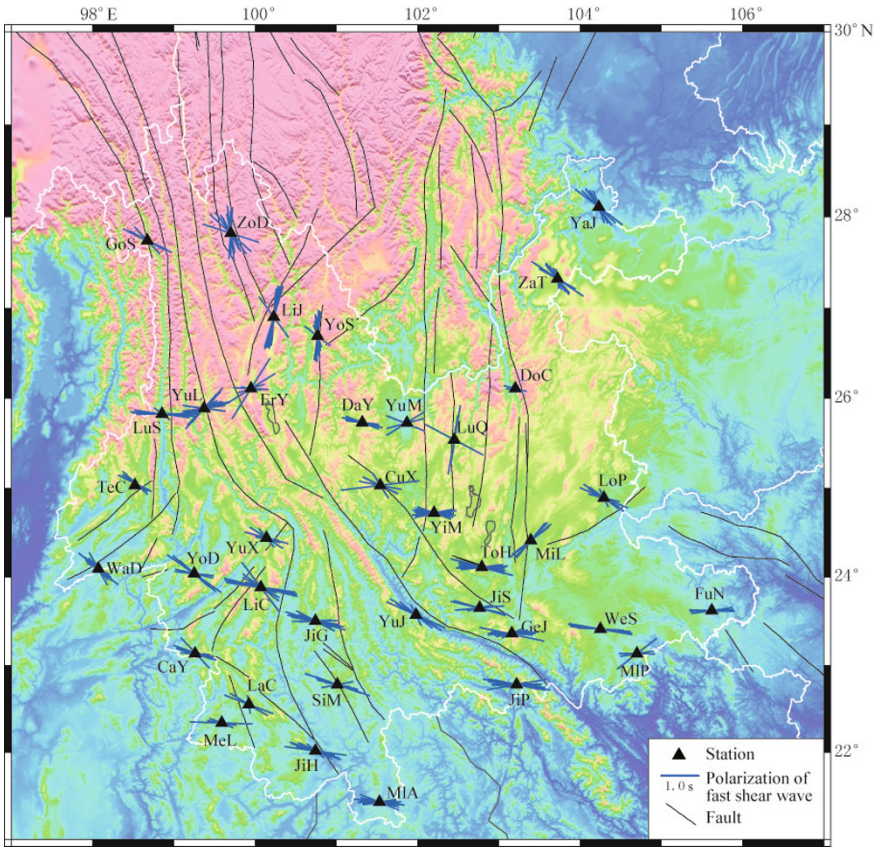

Figure 6 Shear-wave splitting measurements from individual XKS phases in Yunnan area. The orientation of the bars represents the fast polarization direction, and the length is proportional to the splitting time. Triangles are stations used in the study.

study area show NW-SE fast directions which are subparallel to the major faults. The station-averaged time-delays range from 0.55 s to 1.65 s, with a mean value of 1.17 s. Our results are mostly consistent with those from previous studies (Liu et al., 2001; Wang et al., 2007; Chang et al., 2006).

5 Discussion and conclusions

In order to better understand the deformation of crustal and upper mantle, in this section we compare our shear-wave splitting measurements with results from GPS and other strain-measuring techniques (Wang et al., 2006, 2007; Gan et al., 2004; Wu and Zhang, 2011).

In the crust, the polarization orientations beneath most stations near the faults are consistent with the direction of GPS velocity (Gan et al., 2004), focal mechanism solutions (www.globalcmt.org), and the strike of the active fault. For example, the polarization orientation beneath station CuX, above on the Chuxiong-Tonghai fault, is consistent with strikes of the active fault and also with direction of GPS velocity (Figure 7). This phenomenon is the same as Gao et al. (2011), who found that the polarization orientation of fast shear-wave at station on an active strike-slip fault is consistent with the strike of fault. The polarization orientations beneath some stations (MaL, MiL, JiS) are consistent with the strike of the Xiaojiang fault. However, the polarization orientations observed at some of the stations such as YiM, LuQ and DoC are inconsistent with the strike of the neighboring active faults or regional principal compressive stress direction, which is possibly resulted from complicated crustal structures (Shi et al., 2009).

In the upper mantle, the fast-wave orientation is basically in west-east direction, and the delay times falls into the range from 0.55 s to 1.65 s. All these suggest that the anisotropic layer of the mantle is about from 55 km to 165 km. Under the northeastward force from Indian plate, the relatively slow movement of northwestern part of Qinghai-Xizang (Tibetan) block led to the counter-clockwise rotation of Tibetan block. Because of

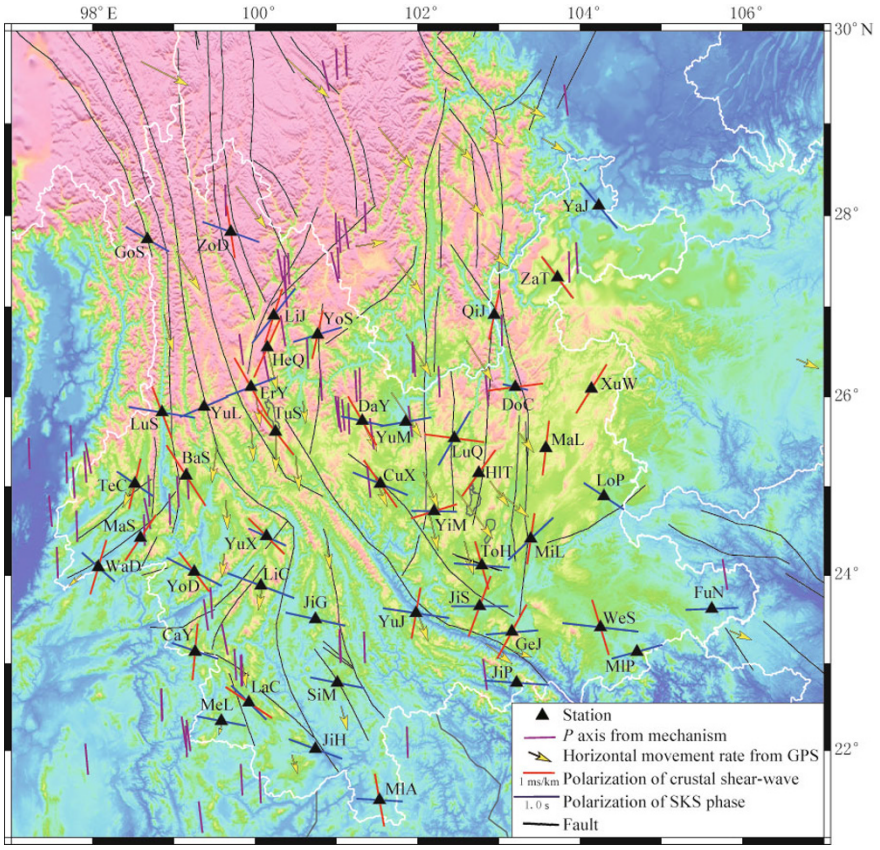

Figure 7 Comparison of maximum horizontal compression direction from focal mechanism solutions and direction of GPS horizontal movement, resulting polarization directions of the fast shear-wave, and strike of faults.

the difference in the movement among the different parts of Tibetan block and its surrounding areas (Wu and Zhang, 2011), the distribution of the active fault and the local stress are anfractuous. In the Qinghai-Xizang (Tibetan) plateau, there is not only the uplift of the vertical deformation, but also the migration of mantle material toward southeast. The directions of fast shear-wave beneath every station are not unanimous. Therefore, it is possible that the distribution of anisotropic characteristics is related to the local fault and stress distribution. The orientations of fast shear-wave do not correlate with direction of GPS velocity field and mechanism of local earthquake. The research result implies that, under the collision of the India and Eurasia plates, the movement of mantle material possibly rotates below Yunnan area. This result is in accordance with studies of Wang et al. (2007) and Wu and Zhang (2011).

The average polarizations of fast shear-waves of S phase and XKS phase beneath 27 stations demonstrate the pattern of crust-mantle deformation (Figure 8). Strong crust-mantle coupling model exists in the internal plateau, and decoupling pattern of crust-mantle deformation indwells in the Yunnan area, southeast edge of Tibetan plateau (Chang et al., 2006; Wang et al., 2007). The polarization orientation obtained from shear-wave splitting of local earthquake indicates the orientation of the principal compressive stress, while the XKS data indicate the maximum extensional or simple shear direction. The two orientations of fast shear-wave could be different, even perpendicular to each other. However, the difference in the orientations of fast shear-wave between XKS phases and S phases of local earthquakes does not convincingly explain vertically inconsistent deformation. The mechanism of different fast polarization orientations of two anisotropic data still needs more studies and verifications.

The Yunnan area is strongly influenced by the Eurasian plate and the Indian plate. It results in complex geophysical and geological patterns. According to the shear-wave splitting researches of local earthquakes, the polarization orientation of the fast

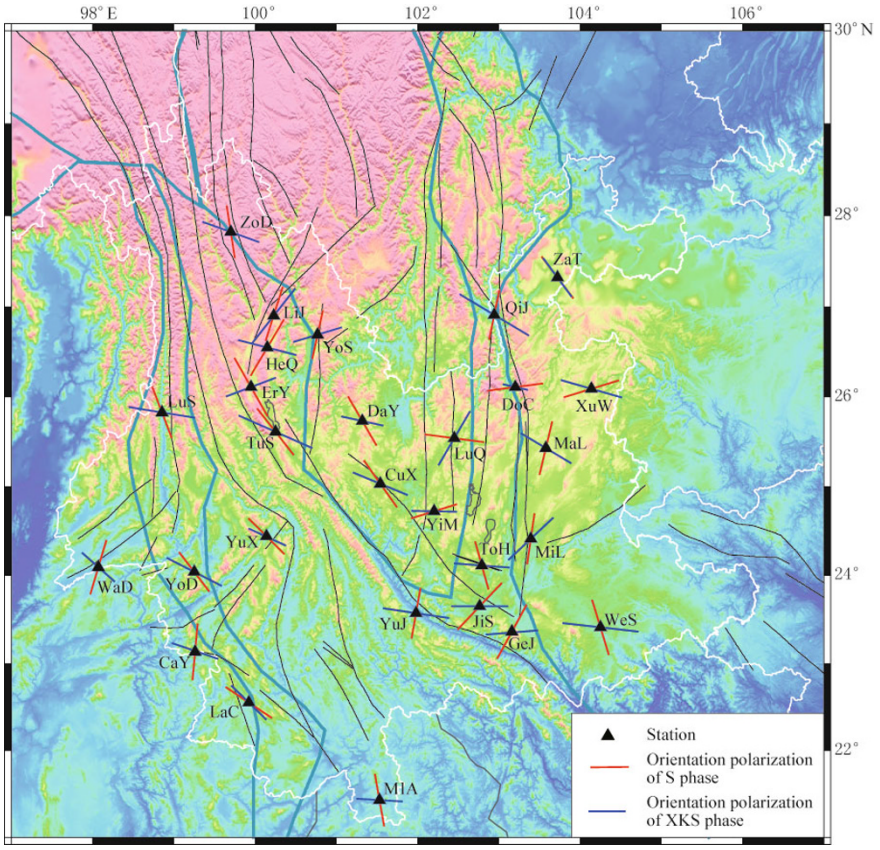

Figure 8 Fast polarization directions from local (red) and teleseismic (blue) shear waves.

shear-wave is consistent with the direction of the local principal compressive stress. However, it is also influenced by the fault distribution and the geologic structure. Thus, we propose that complex local structure could make the fast shear-wave polarization scattered. Using the teleseismic XKS phases, the obtained unanimous polarization orientation and the time-delay beneath each station demonstrate that the mantle material movement is in nearly west-east direction below Yunnan area.

Acknowledgements Many thanks to Professor Stephen Gao for valuable comments and suggestion. Waveform data for this study are provided by Data Management Center of China National Seismic Network at Institute of Geophysics, China Earthquake Administration, and Earthquake Administration of Yunnan Province. This study is supported by National Natural Science Foundation of China Project (No. 41174042), China National Special Fund for Earthquake Scientific Research in Public Interest (No. 201008001) and Basic Research Project of Institute of Earthquake Science, CEA (No. 2009-21).

References

Chang L J, Wang C Y and Ding Z F (2006). A study on SKS splitting beneath the Yunnan region. *Chinese J Geophys* **49**(1): 197–204 (in Chinese with English abstract).

Crampin S (1978). Seismic-wave propagation through a cracked solid: polarization as a possible dilatancy diagnostic. *Geophys J R astr Soc* **53**: 467–496.

Crampin S (1984). An introduction to wave propagation in anisotropic media. *Geophys J R astr Soc* **76**: 17–28.

Crampin S and Atkinson B K (1985). Microcracks in the Earth's crust. *First Break* **3**(3): 16–20.

Deng Q D, Zhang P Z and Ran Y K (2002). Basic characteristics of active tectonics of China. *Science in China* (*Series D*) **32**(12): 1 020–1 030 (in Chinese with English abstract).

Gan W J, Shen Z K and Zhang P Z (2004). Horizontal crustal movement of Tibetan from GPS measurements. *J Geodesy Geodyn* **24**(1): 29–35 (in Chinese with English abstract).

Gao S S, Davis P M, Liu K H, Slack P D, Zorin Y A, Mordvinova V V, Kozhevnikov V M and Meyer R P (1994). Seismic anisotropy and mantle flow beneath the Baikal rift zone. *Nature* **371**: 149–151, doi:10.1038/371149a0.

Gao S S and Liu K H (2009). Significant seismic

anisotropy beneath the southern Lhasa Terrane, Tibetan Plateau. *Geochemistry Geophysics Geosystems* **10**: Q02008, doi:10.1029/2008GC002227.

Gao Y and Crampin S (2004). Observations of stress relaxation before earthquakes. *Geophys J Int* **157**(2): 578–582.

Gao Y, Liu X Q, Liang W and Hao P (2004). Systematic analysis method of shear-wave splitting: SAM software system. *Earthquake Research in China* **18**(4): 365–372.

Gao Y, Wu J, Fukao Y, Shi Y T and Zhu A L (2011). Shear-wave splitting in the crust in North China: stress, faults and tectonic implications. *Geophys J Int* **187**(2): 642–654, doi:10.1111/j.1365-246X.2011.05200.x.

Gao Y, Zheng S H and Sun Y (1995). Crack-induced anisotropy in the crust from shear wave splitting observed in Tangshan region, North China. *Acta Seismologica Sinica* **8**(3): 351–363.

Gao Y, Zheng S H and Zhou H L (1999). Polarization patterns of fast shear wave in Tangshan region and their variations. *Chinese J Geophys* **42**(2): 228–232 (in Chinese with English abstract).

Han R J, Wang S J, Huang K and Song W (1983). Modern stress field and relative motion of intraplate block in southwestern China. *Seismology and Geology* **5**(2): 79–90.

Han R J, Zhang S L and Yan F T (1977). Study on the current tectonic stress field and the characteristics of current tectonic activity in southwest China. *Chinese J Geophys* **20**(2): 96–109.

Hess H H (1964). Seismic anisotropy of the uppermost mantle under oceans. *Nature* **203**: 629–631.

Kind R, Kosarev G L, Makeyeva L I and Vinnik L P (1985). Observations of laterally inhomogeneous anisotropy in the continental lithosphere. *Nature* **318**: 358–361.

Lei J, Wang P D, Yao C and Chen Y T (1997). The near-field shear wave splitting and its relation with structure in Jianchuan, Yunnan Province. *Chinese J Geophys* **40**(6): 792–801.

Liu K, Zhang Z J, Hu J F and Teng J W (2001). Frequency related shear wave splitting and its significance in Chinese mainland. *Science in China* (*Series D*) **31**(2): 155–161.

Liu K H (2009). A uniform database of teleseismic shear-wave splitting measurements for North America. *Geochemistry Geophysics Geosystems* **10**: Q05011, doi:10.1029/2009GC002440.

Liu K H, Gao S S, Gao Y and Wu J (2008). Shear-wave splitting and mantle flow associated with the deflected Pacific slab beneath northeast Asia. *J Geophys Res* **133**: B01305, doi:10.1029/2007JB005178.

Savage M K (1999). Seismic anisotropy and mantle deformation: What have we learned from shear wave splitting? *Rev Geophys* **37**: 65–106.

Shi Y T, Gao Y, Wu J and Su Y J (2009). Crustal seismic anisotropy in Yunnan, southwestern China. *J Seism* **13**(2): 287–299.

Silver P G (1996). Seismic anisotropy beneath the continents: Probing the depths of geology. *Annual Rev Earth Planet* **24**: 385–432.

Silver P G and Chan W W (1991). Share-wave splitting and subcontinental mantle deformation. *J Geophys Res* **96**: 16 429–16 454.

Vinnik L P, Green R W E and Nicolaysen L O (1995). Recent deformations of the deep continental root beneath Southern Africa. *Nature* **375**: 50–52.

Wang C Y, Chang L J, Lu Z Y, Qin J Z, Su W, Silver P G and Flesch L (2007). Seismic anisotropy of upper mantle in eastern Tibetan Plateau and related crust-mantle coupling pattern. *Science in China* (*Series D*) **50**(8): 1 150–1 160 (in Chinese with English abstract).

Wang C Y, Wu J P and Lou H (2006). Study of crustal and upper mantle's structure and mantle deformation field beneath the eastern Tibetan plateau. *Earth Science Frontiers* **13**(5): 349–359 (in Chinese with English abstract).

Wolfe C J and Silver P G (1998). Seismic anisotropy of oceanic upper mantle: Shear wave splitting methodologies and observations. *J Geophys Res* **103**(B1): 749–771.

Wu J and Zhang Z J (2011). Spatial distribution of seismic layer, crustal thickness, and v_P/v_S ratio in the Permian Emeishan Mantle Plume region. *Gondwana Research* doi:10.1016/j.bbr.2011.03.031.

Wu J P, Ming Y H and Wang C Y (2001). The S wave velocity structure beneath digital seismic stations of Yunnan province inferred from teleseismic receiver function modeling. *Chinese J Geophys* **44**(2): 228–237 (in Chinese with English abstract).

Wu J P, Ming Y H and Wang C Y (2004). Source mechanism of small-to-moderate earthquake and tectonic stress filed in Yunnan province. *Acta Seismological Sinica* **17**(5): 509–517, doi:10.1007/s11589-004-0032-2.

Zhang Z J, Teng J W, Badal J and Liu E R (2009). Construction of regional and local seismic anisotropic structures from wide-angle seismic data: crustal deformation in the southeast of China. *Journal of Seismology* **13**: 241–252.

Zheng X F, Chen C H and Zhang C H (2008). Study on temporal variations of shear-wave splitting in the Chiayi area, aftershock zone of 1999 Chichi earthquake, Taiwan. *Chinese J Geophys* **51**(1): 149–157 (in Chinese with English abstract).

Zheng X F, Yao Z X, Liang J H and Zheng J (2010). The role played and opportunities provided by IGP DMC of China National Seismic Network in Wenchuan earthquake disaster relief and researches. *Bull Seismol Soc Am* **100**(5B): 2 866–2 872.